High Performance Amorphous Polymeric Thin-Film Transistors Based on Poly[(1,2-bis-(2′-thienyl)vinyl-5′,5″-diyl)-*alt*-(9,9-dioctylfluorene-2,7-diyl] Semiconductors

Dae Sung Chung,[†] Sung Joong Lee,[‡] Jun Woo Park,[†] Dan Bi Choi,[†] Dong Hoon Lee,[†] Jong won Park,[§] Sung Chul Shin,*[,‡] Yun-Hi Kim,[‡] Soon-Ki Kwon,*[,§] and Chan Eon Park*[,†]

Polymer Research Institute, Department of Chemical Engineering, Pohang University of Science and Technology, Pohang, 790-784, Korea, , Deaprtment of Chemistry & RINS, Gyeongsang National University, Jinju, 660-701, Korea, and, School of Nano & Advanced Materials Science and Engineering and ERI, Gyeongsang National University, Jinju, 660-701, Korea

Received February 16, 2008. Revised Manuscript Received March 10, 2008

We have synthesized a new p-type polymer, poly[(1,2-bis-(2′-thienyl)vinyl-5′,5″-diyl)-*alt*-(9,9-dioctyldecylfluorene-2,7-diyl] (PTVTF), via a Suzuki coupling reaction. PTVTF was found with UV–vis absorption spectroscopy, GIXD, AFM, and NEXAFS to be an 'annealing-free' amorphous polymer. Despite its amorphous nature, our time-of-flight measurements demonstrate that PTVTF is a good hole transport material with an intrinsic hole mobility of 2×10^{-4} cm^2/Vs, which is comparable to those of crystalline polymers such as P3HT. A solution-processed PTVTF FET with a bottom gate/top contact geometry was found to exhibit good device performance with superior reproducibility. The field-effect mobility of holes was found to be 2×10^{-2} cm^2/Vs with a good subthreshold swing of 1.7 Vdecade^{-1}. The output characteristics indicate that good saturation and ohmic contact are present. The amorphous nature of PTVTF makes it a very promising candidate for commercial OTFTs since its properties are independent of fabrication conditions. From the temperature dependence of the mobility of amorphous PTVTF, we found that increases in the hydrophobicity of the dielectric substrate improve the mobility of PTVTF by reducing the trap density of the semiconductor layer.

Introduction

Polymer-based organic field-effect transistors (OFETs) have a number of advantages over traditional thin-film transistors (TFTs) based on inorganic materials, including chemical tunability, compatibility with plastic substrates, structural flexibility, and solution processing, so they have recently been intensively studied.[1–5] The characteristics and processability of OTFTs mean that they could be fabricated at low cost for use in various electronic devices, such as smart cards, sensors, electronic paper, memory devices, radio frequency identification (RFID) tags, and the driving circuits of large-area displays.[6–11]

Nevertheless, despite remarkable recent progress, the field-effect transistor (FET) mobilities of polymeric semiconductors remain far lower than those of their inorganic counterparts. For practical applications, these polymeric semiconductors should provide FET mobilities close to that of amorphous silicon.[6,12] The establishment of a particular molecular alignment was thought to be essential for high carrier mobilities because the charge carrier in polymeric semiconductors is transported by hopping.[7,10,12] A crucial method for achieving highly ordered alignments of solid-state semiconductor molecules is self-assembly *via* face-to-face stacking (cofacial π-stacking), which can contribute to efficient $\pi-\pi$ coupling and thus increase mobility.[13,14]

* (S.C.S.) E-mail: scshin@gnu.ac.kr, tel: +82-55-751-6022, fax: +82-55-751-0244; (S.K.W.) e-mail:skwon@gnu.ac.kr, tel: +82-55-751-6022, fax: +82-55-751-0244; (C.E.P.) cep@postech.ac.kr, tel: +82-54-279-2269, fax: +82-54-279-8298. Dae Sung Chung and Sung Joong Lee contributed equally to this work.

[†] Pohang University of Science and Technology.

[‡] Department of Chemistry & RINS, Gyeongsang National University.

[§] School of Nano & Advanced Materials Science and Engineering and ERI, Gyeongsang National University.

(1) Sirringhaus, H. *Adv. Mater.* **2005**, *17*, 2411–2425.
(2) Chabinyc, M. L.; Salleo, A. *Chem. Mater.* **2004**, *16*, 4509–4521.
(3) Dimitrakopoulos, C. D.; Malenfant, P. R. L. *Adv. Mater.* **2002**, *14*, 99–117.
(4) Forrest, S. R. *Nature* **2004**, *428*, 911–918.
(5) Meng, H.; Sun, F.; Goldfinger, M. B.; Gao, F.; Londono, D. J.; Marshal, W. J.; Blackman, G. S.; Dobbs, K. D.; Dalen, E.; Keys, D. E. *J. Am. Chem. Soc.* **2006**, *128*, 9304–9305.
(6) Nishide, J.-I.; Oyamada, T.; Akiyama, S.; Sasabe, H.; Adachi, C. *Adv. Mater.* **2006**, *18*, 3120–3124.
(7) Katz, H. E.; Bao, Z.; Gilat, S. L. *Acc. Chem. Res.* **2001**, *34*, 359.
(8) Garnier, F.; Hajlaoui, A.; Yassar, A.; Srivastava, P. *Science* **1994**, *265*, 1684.
(9) Huitena, H. E. A.; Gelinck, G. H.; van der Putter, J. B. P. H.; Kujik, K. E.; Hart, C. M.; Cantatore, E.; Herwig, P. T.; van Breeman, A. J. J. M.; de Leeuw, D. M. *Nature* **2001**, *414*, 599.
(10) Sirringhaus, H.; Tessler, N.; Friend, R. H. *Science* **1998**, *280*, 1741.
(11) Brown, A. R.; Jarret, C. P.; de Leeuw, D. M.; Matters, M. *Synth. Met.* **1997**, *88*, 37.
(12) Ong, B. S.; Wu, Y.; Liu, P.; Gardner, S. *Adv. Mater.* **2005**, *17*, 1141–1144.
(13) Kim, D. H.; Lee, D. Y.; Lee, H. S.; Lee, W. H.; Kim, Y. H.; Han, J. I.; Cho, K. *Adv. Mater.* **2007**, *19*, 678–682.
(14) Li, X.-C.; Sirringhaus, H.; Garnier, F.; Moratti, S. C.; Feeder, N.; Friend, R. H. *J. Am. Chem. Soc.* **1998**, *120*, 2206.

10.1021/cm800447k CCC: $40.75
Published on Web 04/24/2008

Polymers with an extended planar π-conjugated structure that exhibit well-defined crystalline domains are required to achieve such efficient cofacial π-stacking. For example, liquid crystalline polymers such as regioregular head-to-tail poly(3-hexylthiophene)s,[10] poly[5,5′-bis(3-dodecyl-2-thienyl)-2,2′-bithiophene]] (PQT-12),[12] poly(2,5-bis(3-alkylthiophene-2-yl)thieno[3,2-b]thiophene) (PBTTT),[15] and poly(9,9′-n-dioctylfluorene-*alt*-biselenophene) (F8Se2)[26] assemble into a highly ordered architecture (large crystalline domain), and possess an extended planar π-stacked system, resulting in high charge-carrier mobilities. However, to obtain a highly ordered crystalline structure, chain alignment procedures such as rubbing and thermal annealing are necessary. These procedures are often very time-consuming and are hard to optimize with solution processing methods such as spin coating, drop casting, and inkjet printing. Therefore, easily processable, 'annealing-free', and 'fabrication method independent' amorphous polymers are important semiconducting materials for the commercialization of organic field effect transistors. Some groups have reported the fabrication of amorphous small molecule semiconductor materials such as ladder tetraazapentacenes[16] and spiro-linked compounds[17] via vacuum processes. However, the device performances of these materials have been found to be unsatisfactory when compared to those of other vacuum-deposited small molecules and inferior to those of solution-processed polymer–semiconductors. Veres and co-workers reported the fabrication of amorphous polymer–semiconductors consisting of polytriarylamines (PTAA) and used a low-*k* fluoro polymer as the gate dielectric layer to achieve a field-effect mobility close to 10^{-2} cm^2/Vs.[18] The further development of amorphous polymer–semiconductors with high device performance is required. In addition to amorphous characteristics, the polymer must also have an air stable molecular structure because the widely studied regioregular polythiophenes are sensitive to oxidative doping under ambient conditions, resulting in an increased off-current and degraded semiconductor properties and performance.[19,20] The susceptibility of semiconducting polythiophenes to oxidative doping can be suppressed by increasing their ionization potentials (IPs), i.e. by lowering their HOMO levels, which depend on the effective lengths of their π-conjugation.[12,21–23] One strategy for lowering the HOMO level is to insert a nonactive block with a wide HOMO–LUMO band gap such as a fluorene moiety into appropriate positions within the polythiophene backbone, which limits the effective π-conjugation length. The use of this ingenious molecular design consisting of a nonactive block in semiconducting polythiophenes enables the fine-tuning of the π-conjugation so that there is a balance between the desired mobility and oxidation suppression. This approach motivated the preparation in this study of poly[(1,2-bis-(2′-thienyl)vinyl-5′,5″-diyl)-*alt*-(9,9-didecylfluorene-2,7-diyl) (PTVTF) as an amorphous polymer–semiconductor. The π-conjugation length of the α,β-bis(thienyl)vinyl moiety of the polymer, which is the active block, is more extended than in previously reported fluorene-*alt*-bithiophene-based semiconducting copolymers.[24–27] Time of flight measurements were used to show that PTVTF has a high intrinsic charge-carrier mobility, above 2×10^{-4} cm^2/Vs, which is similar to that of crystalline P3HT.[28,29] By using grazing incidence X-ray diffraction, atomic force microscopy, and UV–vis absorption analysis, we confirmed that PTVTF forms an amorphous polymeric layer regardless of the dielectric surface treatment. Near-edge X-ray absorption spectroscopy was carried out to show that various dielectric surface treatments do not affect the molecular orientation at the interface. We fabricated various bottom gate/top contact TFT devices with PTVTF as a semiconductor and found that one of these devices exhibits higher device performances than other amorphous materials: a field-effect mobility of 2×10^{-2} cm^2/Vs and an on/off ratio of 3×10^5 with a good subthreshold swing of 1.7 Vdecade^{-1}. The variation of the device performance with the dielectric surface treatment was also investigated by examining the temperature dependence of the field-effect mobility.

Experimental Section

Preparation of Diethyl [(5-Bromothiophen-2-yl)methyl]phosphonate (1). A 250 mL flask fitted with a reflux condenser was charged with 2-bromothiophene (3.3 g, 100 mmol), paraformaldehyde (3.3 g, 110 mmol), and HOAc (50 mL). HBr in HOAc (20 mL, 37%) was added, and the solution was heated in a well ventilated fume cupboard at 50 °C for 3 h. After cooling, the reaction mixture was extracted with CH_2Cl_2 (200 mL) and washed with cold H_2O (50 mL). After standard workup, 20 g of a brown oil were isolated and mixed with triethyl phosphite (14 mL, 80 mmol). The viscous solution was stirred at 150 °C overnight and the excess triethyl phosphite was evaporated to produce a crude dark oil. Chromatographic separation on silica gel was achieved using 5 g portions of the oil (Et_2O). The product was isolated as a red oil (15 g, 48% overall). ^{1}H NMR (300 MHz, $CDCl_3$) δ [ppm]

(15) Mcculloch, I.; Heeney, M.; Bailey, G.; Genevicius, K.; Macdonald, I.; Shkunov, M.; Sparrowe, D.; Tierney, S.; Wagner, R.; Zhang, W.; Chabinyc, M. L.; Kline, R. J.; Mcgehee, M. D.; Toney, M. F. *Nat. Mater.* **2006**, *5*, 328–333.
(16) Ma, Y.; Sun, Y.; Liu, Y.; Gao, J.; Chen, S.; Sun, X.; Qiu, W.; Yu, G.; Cui, G.; Hu, W.; Zhu, D. *J. Mater. Chem.* **2005**, *15*, 4894.
(17) Saragi, T. P. I.; Fuhrmann-Lieker, T.; Salbeck, J. *Synth. Met.* **2005**, *148*, 267.
(18) Veres, J.; Ogier, S. D.; Leeming, S. W.; Cupertino, D. C.; Khaffaf, S. M. *Adv. Funct. Mater.* **2003**, *13*, 199.
(19) Li, W.; Katz, H. E.; Lovinger, A. J.; Laquindanum, J. G. *Chem. Mater.* **1999**, *11*, 458.
(20) Meijer, E. J.; Detcheverry, C.; Baesjou, P. J.; van Veenendaal, E.; de Leeuw, D. M.; Klapwijk, T. M. *J. Appl. Phys.* **2003**, *93*, 4831.
(21) Ong, B.; Wu, Y.; Jiang, L.; Liu, P.; Murti, K. *Synth. Met.* **2004**, *142*, 49.
(22) Liu, P.; Wu, Y.; Li, Y.; Ong, B. S.; Zhu, S. *J. Am. Chem. Soc.* **2006**, *128*, 4554.
(23) Li, Y.; Wu, Y.; Liu, P.; Birau, M.; Pan, H.; Ong, B. S. *Adv. Mater.* **2006**, *18*, 3029.
(24) Sirringhaus, H.; Brown, P. J.; Friend, R. H.; Nielsen, M. M.; Bechgaard, K.; Langeveld-Voss, B. M. W.; Spiering, A. J. H.; Janssen, R. A. J.; Meijer, E. W.; Herwig, P.; de Leeuw, D. M. *Nature* **1999**, *401*, 685.
(25) Sirringhaus, H.; Wilson, R. J.; Friend, R. H.; Inbasekaran, M.; Wu, W.; Woo, E. P.; Grell, M.; Bradley, D. D. C. *Appl. Phys. Lett.* **2000**, *77*, 406.
(26) Lim, E.; Jung, B.-J.; Lee, J.; Shim, H.-K.; Lee, J.-I.; Yang, Y. S.; Do, L.-M. *Macromolecules* **2005**, *38*, 4531.
(27) Lim, E.; Kim, Y. M.; Lee, J.-I.; Jung, B.-J.; Cho, N. S.; Lee, J.; Do, L.-M.; Shim, H.-K. *J. Polym. Sci.: Part A: Polym. Chem.* **2006**, *44*, 4709.
(28) Malhotra, B. D.; Tkashima, W.; Pandey, S. S.; Singhal, R.; Endo, K.; Rikukawa, M.; Kaneto, K. *Jpn. J. Appl. Phys.* **1999**, *38*, 6768.
(29) Kaneto, K.; Hatae, K.; Nagamatsu, S.; Takashima, W.; Pandey, S. S.; Endo, K.; Rikukawa, M. *Jpn. J. Appl. Phys.* **1999**, *38*, L1188.

6.8 (d, 1H, $J = 3.8$ Hz), 6.62 (t, 1H, $J = 3.8$ Hz), 4.0 (dq, 4H), 3.2 (d, 2H, $J = 20.8$ Hz), 1.2 (t, 6H, $J = 7.1$ Hz); ^{13}C NMR ($CDCl_3$) 134, 130, 128, 104, 64, 28, 16.

Preparation of 1,2-(*E*)-Bis(5′-bromo-2′*C*-thienyl)ethene (2). Sodium hydride (571 mg, 23.9 mmol) was added to a solution of 5-bromo-2-thiophenecarboxaldehyde (2.46 g, 12.9 mmol) and diethyl [(5-bromothiophen-2-yl)methyl]phosphonate (4.00 g, 12.8 mmol) in DME (40 mL), which resulted in effervescence and a change in color to yellow. This solution was heated at 60 °C for 23 min. The mixture was extracted with ethyl acetate (2 × 20 mL), and the combined organic extracts were washed with a saturated solution of NaCl, dried with $MgSO_4$, and filtered. The solute was collected and evaporated using a rotary evaporator. Further purification with column chromatography on silica gel using a CH_2Cl_2/hexane (1:1) eluent followed by recrystallization from MeOH gave a pale yellow crystalline solid, which was identified as 1,2-(*E*)-bis(5′ -bromo-2′-thienyl)ethene (2.54 g, 58%): mp 105–106 °C; ^{1}H NMR (300 MHz, $CDCl_3$) δ [ppm] 6.95 (d, 2H, $J = 3.1$ Hz), 6.82 (s, 2H), 6.78 (d, 2H, $J = 3.1$ Hz); ^{13}C NMR ($CDCl_3$) 143.5, 130.6, 126.6, 121.1, 111.5: MS (EI) 350 ($[M]^+$, 70), 271 ($[M\text{-}Br]^+$, 10), 190 ($[M - 2Br]^+$, 100).

Preparation of 2,7-Bis(4,4,5,5-tetramethyl-1,3,2-dioxaborolan-2-yl)-9,9-dioctylfluorene (3). 2,7-Dibromo-9,9-dioctylfluorene (6 g, 10.9 mmol) was dissolved in 150 mL of anhydrous THF in a 250 mL flask and cooled to –78 °C in an ethyl acetate/N_2 ice bath. A 10.9 mL amount of 2.5 M n-butyllithium (27.4 mmol) was added slowly to this solution, which was then stirred for 40 min. A 5.6 mL amount of 2-isopropoxy-4,4,5,5-tetramethyl-1,3,2-dioxaborolane (27.4 mmol) was then added, and the reaction mixture was allowed to warm slowly to room temperature. The reaction was stirred overnight and then quenched with brine; the product was extracted into Et_2O, washed again with brine, and dried over $MgSO_4$. After removal of the solvent, the resulting boronic ester was recrystallized from hexane to give a white solid (yield 50%): mp 123–124 °C; ^{1}H NMR (300 MHz, $CDCl_3$) δ [ppm] 7.82 (d, 2H), 7.76 (s, 2H), 7.35 (d, 2H), 2.01 (m, 4H), 1.41 (s, 24H, CH3), 1.22–1.02 (m, 20H), 0.83 (t, 6H), 0.56 (m, 4H).

Preparation of Poly[(1,2-bis(2′-thienyl)vinyl-5′,5″-diyl)-*alt*-(9,9-dioctylfluorene-2,7-diyl)] (4). Tetrakis(triphenylphosphine-)palladium ($Pd(PPh_3)_4$) (0.09 g, 0.078 mmol) was added to a mixture of 1,2-(*E*)-bis(5′*C*-bromo-2′-thienyl)ethene (0.54 g, 1.56 mmol), 2,7-bis(4,4,5,5-tetramethyl-1,3,2-dioxaborolan-2-yl)-9,9-dioctylfluorene (1.00 g, 1.56 mmol), 2 M K_2CO_3 (5 mL), and anhydrous toluene (30 mL) under a nitrogen atmosphere. After the reaction mixture was refluxed for 28 h, 2-bromonaphthalene was added with small amounts of catalysts for end-capping. The reaction mixture was then poured into a solution of 2% HCl and MeOH. Finally, the crude polymer was dissolved in $CHCl_3$ followed by the addition of MeOH to afford the desired polymer. The product was an orange solid (0.58 g): ^{1}H NMR (300 MHz, $CDCl_3$) δ [ppm] 7.69 (d, 2H), 7.60 (t, 4H), 7.30 (d, 2H), 7.06 (d, 2H), 7.03 (d, 2H), 2.04 (s, 4H), –1.02 (m, 20H), 0.83 (t, 6H), 0.56 (m, 4H). (m, 6H); ^{13}C NMR (300 MHz, $CDCl_3$) 151.80, 143.80, 141.73, 140.35, 133.09, 127.54, 124.71, 123.57, 121.40, 120.20, 119.78, 55.30, 40.43, 31.83, 30.01, 29.24, 23.79, 22.63, 14.10.

Time of Flight. Semitransparent aluminum (Al) layers of 20 nm thickness were deposited as bottom electrodes on glass substrates with thermal evaporation. For the preparation of thick drop-cast PTVTF films (~9 μm), PTVTF solution (3 wt% in chloroform) was poured into a template of Al foil on each bottom electrode and vacuum-dried at 60 °C for 24 h. The thickness and the flatness of the drop-cast P3HT films were measured using an alpha-stepper (Alpha Step 500, Tencor). Thin Al layers (20 nm) were deposited as the top electrode on the prepared P3HT films to complete the devices. ToF experiments were performed in a vacuum cryogenic chamber. The ToF photocurrent transients were obtained by illuminating the samples with N_2 laser (337 nm) pulses of duration 6 ns under a dc bias.

Morphology and Structure Characterization. UV–vis measurements were carried out on a UV–vis-NIR spectrophotometer (Cary 5000, Varian Co.). Synchrotron X-ray diffraction analyses of the PTVTF films were performed at the 10C1 beam line (wavelength ~ 1.54 Å) of the Pohang Accelerator Laboratory (PAL). AFM (Multimode IIIa, Digital Instruments) operating in tapping-mode was used to image the surface morphology of the PTVTF thin films.

Film Orientation Characterization. NEXAFS spectroscopy was used to determine the orientation of the PTVTF backbone chains. The thin PTVTF films (~20 nm) were investigated using the photoemission spectroscopy beam line 4B1 at the Pohang Accelerator Laboratory (PAL).

Fabrication of the OFET Devices. Top contact OFETs were fabricated on a common gate of highly n-doped silicon with a 300 nm thick thermally grown SiO_2 dielectric layer. To produce hydrophobic dielectric surfaces, hexamethyldisilazane (HMDS), octyltrichlorosilane (OTS), octadecyltrichlorosilane (ODTS), and polydimethylsiloxane (PDMS) layers were coated onto the SiO_2 dielectric layer. Films of the organic semiconductor were spin coated at 2000 rpm from a 0.7 wt% chloroform solution, with a nominal thickness of 45 nm. Gold source and drain electrodes were evaporated with a shadow mask on top of each semiconductor (100 nm). In all the measurements, we used channel lengths (L) of 100 μm and channel widths (W) of 2000 μm. The electrical characteristics of the FETs were measured in air using Keithley 2400 and 236 source/measure units. The field-effect mobilities were extracted in the saturation regime from the slopes of the source-drain currents.

Results and Discussion

Synthesis. The synthesis of PTVTF (poly[(1,2-bis-(2′-thienyl)vinyl-5′,5″-diyl)-*alt*-(9,9-dioctylfluorene-2,7-diyl)]) is described in Scheme 1. 1,2-(*E*)-Bis(5′-bromo-2′-thienyl)ethene **2** was prepared from 2-bromothiophene via a Wittig reaction in a yield of approximately 58%. The Suzuki coupling reaction was employed in the polymerization of PTVTF. After polymerization, end-capping was carried out with 2-bromonaphthalene. The Soxhlet extraction of the crude polymer to remove oligomeric materials afforded PTVTF an orange color in a yield of 60%. The structure of the obtained PTVTF was confirmed with ^{1}H NMR, ^{13}C NMR, and IR spectroscopy. The signals near 2.04–0.78 and 7.06 ppm were assigned to the protons connected to the octyl groups in the fluorene units and the vinylene groups, respectively. PTVTF was found to be highly soluble in most organic solvents such as methylene chloride, chloroform, toluene, and *o*-dichlorobenzene. The PTVTF was found with gel permeation chromatography (GPC) analysis to have a number-average molecular weight (M_n) of 11 325 g/mol with a polydispersity index of 2.10 with respect to a polystyrene standard. The thermal stability of PTVTF was evaluated with thermogravimetric analysis (TGA) under a nitrogen atmosphere. The polymer was found to exhibit very good thermal stability up to 420 °C.

Time of Flight. Figure 1 shows the current–voltage characteristics of the PTVTF films at various bias voltages. We can easily calculate the drift mobilities using the equation

Scheme 1. Synthetic Route for PFTVT[a]

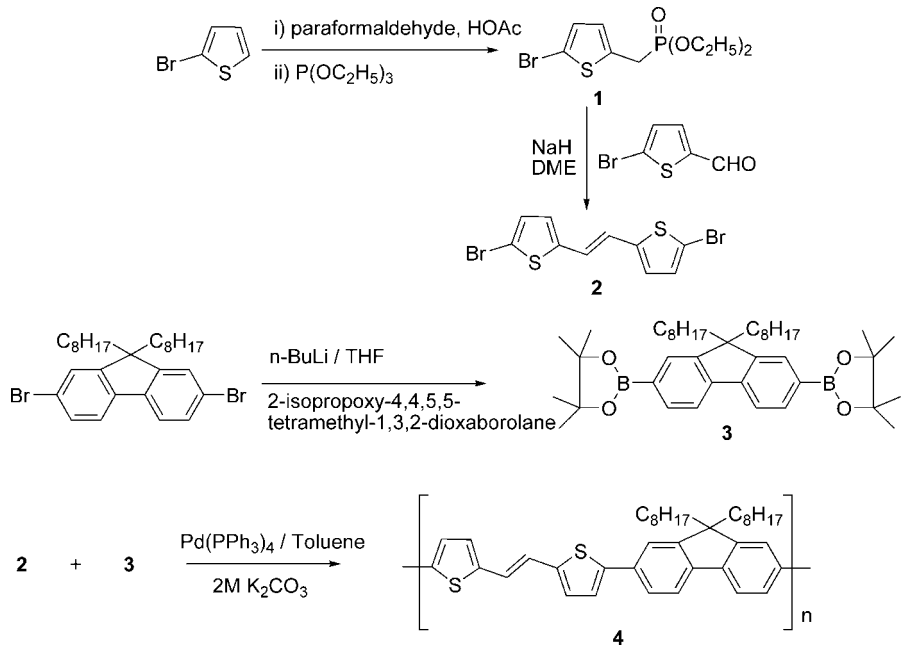

[a] The synthetic procedures used for **1**−**3** are as described in the literature.

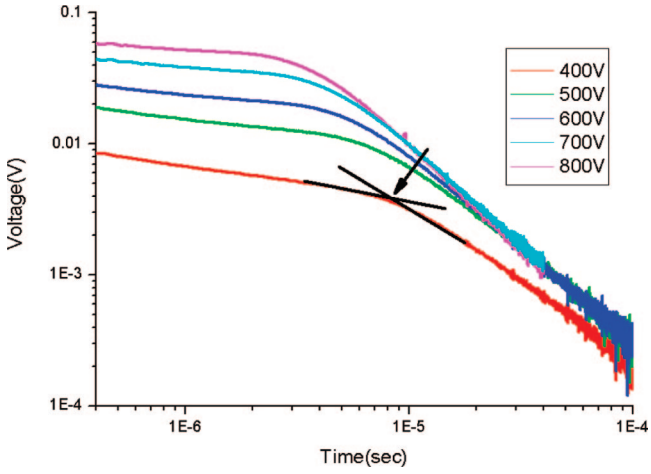

Figure 1. Time of flight photocurrent transients for PFTVT (~9 μm) at room temperature for various applied voltages.

$\mu = \frac{d^2}{Vt}$ from the kinks shown in Figure 1, where d is the thickness of the film, V is the applied dc bias voltage, and t is the measured transit time. The time-of-flight mobility was found to be $2-5 \times 10^{-4}$ cm^2/Vs at bias voltages ranging from 200 V to 500 V, which is similar to those of well-known conducting polymers such as P3HT. This result shows that PTVTF is a good hole transport material despite the presence of the inserted nonactive fluorene moiety block with a wide HOMO–LUMO gap.

Amorphous Structure and Morphology. We prepared five kinds of dielectric surfaces by carrying out various treatments to produce untreated and HMDS-, OTS-, ODTS-, and PDMS-treated SiO_2 dielectrics. The water contact angles of the dielectrics were found to be 25 ± 2° (untreated), 68 ± 2° (HMDS), 99 ± 2° (OTS), 108 ± 1° (ODTS), and 109 ± 1° (PDMS). We deposited PTVTF on these dielectric surfaces and investigated the variations in their thin film structures and morphologies. Figure 2a shows the UV–vis absorption spectroscopy results for PTVTF spin-coated onto the five different dielectric surfaces and for PTVTF solution in chloroform. The absorption spectra of all the spin-coated films have undergone a very subtle red shift with respect to that of the solution state. In addition, there are no significant changes in the absorption peaks of the spin-coated films as a result of thermal annealing at various temperatures (Figure 2b). This result indicates that PTVTF is an amorphous polymer. In order to confirm that PTVTF is amorphous, we performed grazing incidence X-ray diffraction (GIXD). The in-plane GIXD patterns in Figure 3 of PTVTF spin-coated onto OTS-treated dielectric surfaces that were thermally annealed at various temperatures (inset: the out-of-plane GIXD pattern) contain no Bragg refraction peaks, confirming their amorphous state.[30] As shown in Figure 4, the AFM height images of PTVTF spin-coated onto the various dielectric surfaces confirm that PTVTF has an amorphous structure. Furthermore, the thermal annealing of PTVTF at various temperatures does not alter the morphology of PTVTF and does not result in any endothermic and exothermic peaks in the results of differential scanning calorimetry (DSC, not shown here).

OTFT Characteristics. Despite its amorphous nature, the PTVTF thin film transistors were found to exhibit typical transfer and output curves, as shown in Figure 5. The output behaviors are characteristic of the metal oxide FET gradual-channel model with good saturation and ohmic contact. The transfer characteristics are satisfactory, with a subthreshold slope of 1.7 V decade^{-1}, a threshold voltage of –10 V, and a field-effect mobility of 0.02 cm^2/Vs. Discrepancy between TOF and FET mobility by 2 orders of magnitude is thought to be originated from the difference of charge carrier density.

(30) Alexander, L. E. *X-Ray Diffraction Methodsin Polymer Science*; John Wiley: New York,1969; p 43.

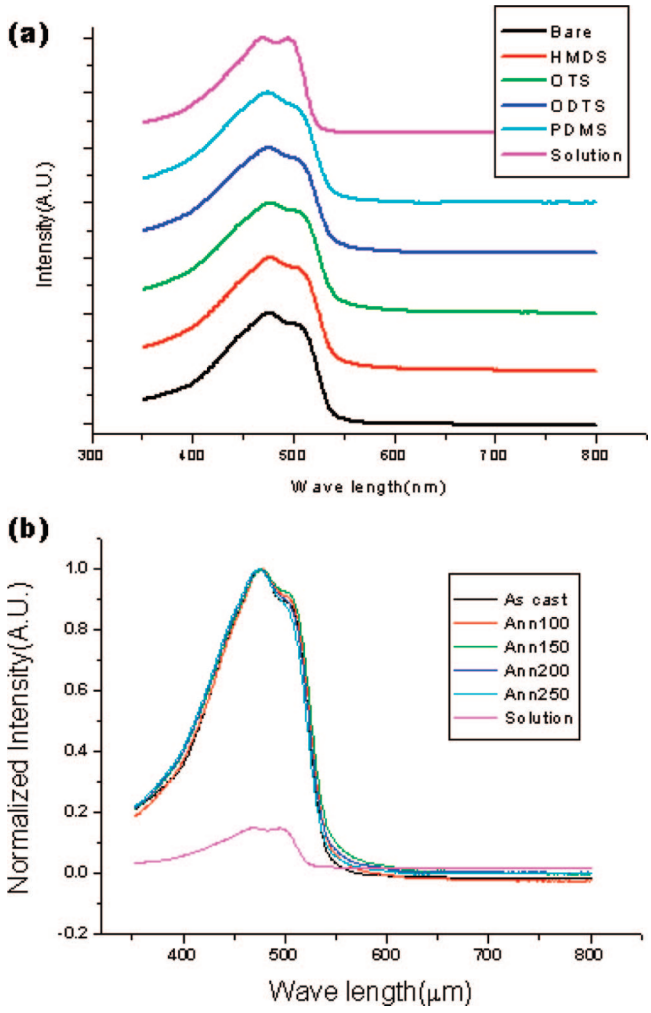

Figure 2. (a) UV–visible absorption spectra of PFTVT spin-coated onto various dielectric surfaces and of PFTVT solution in chloroform, and (b) UV–visible absorption spectra of PFTVT spin-coated onto OTS-treated substrates that were thermally annealed at various temperatures: 100, 150, 200, and 250 °C.

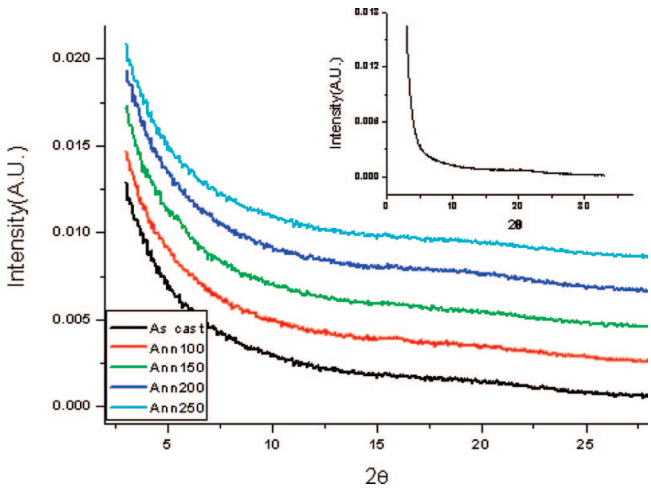

Figure 3. In-plane grazing incidence XRD data for PFTVT spin-coated onto OTS-treated thermally annealed dielectric surfaces (inset: out-of-plane grazing incidence XRD).

In the case of FET, negative gate bias accumulates positive charge carrier near the channel region, thereby inducing high charge carrier density compared with the hole-only diode device.[37] Furthermore the performance of the amorphous PTVTF OTFTs does not vary with the variation in the device fabrication method because of the amorphous nature of PTVTF. However, the OTFT device characteristics of PTVTF are still inferior to those of well-known crystalline semiconductor materials.[12,15] Notwithstanding the lower mobility of the PTVTF OTFTs, the amorphous nature of PTVTF and the good reproducibility of its devices enable its application in low cost, large-area electronics such as E-papers because it can be fabricated without annealing.

Although the structure and morphology of the PTVTF thin films were found to be independent of the dielectric surface treatment, the field-effect mobility was found to be strongly correlated with the dielectric surface treatment (Figure 6). A high field-effect mobility above 10^{-2} cm^2/Vs appeared only when a hydrophobic dielectric surface was used. As the hydrophobicity of the dielectric surface decreases, there is a clear downward trend in the field-effect mobility. The surface orientation of PTVTF on each dielectric surface was examined with near-edge X-ray absorption fine-structure spectroscopy (NEXAFS). Figure 7 shows a series of NEXAFS spectra obtained at room temperature for two different incidence angles, 90° and 20°. The spectra are composed of four main peaks: C=C 1s $\rightarrow\pi^*$ at 285.5 eV, superimposed C−H and C−S 1s $\rightarrow\sigma^*$ at 288.1 eV, C−C 1s $\rightarrow\sigma^*$ at 293.5 eV, and C=C 1s $\rightarrow\sigma^*$ at 303.7 eV. These peak positions are consistent with previously observed NEXAFS spectra for polyfluorene or polythiophene films.[32–34] It is hard to differentiate the PTVTF side chains of the semiconductor layer from the alkyl chains of the surface treatment layer by using the NEXAFS peaks originating only from C−C or C−H bonds. Since the intensity of the peak for the C=C 1s $\rightarrow\pi^*$ transition at normal X-ray incidence (90°) is greater than that at grazing X-ray incidence (20°) and the reverse is true of the peak for the C=C 1s $\rightarrow\sigma^*$ transition, the majority of the PTVTF backbone appears to be faced to the dielectric surface. For clarity, the difference spectra (90° − 20°) for all NEXAFS data are presented in Supporting Information. Therefore, we can conclude that PTVTF thin film is not truly isotropic but has some orientational preference for retaining a high degree of disorder, as derived from the XRD and NEXAFS study. However the spectra in the presence of the various surface treatment layers are still very similar, meaning that the dependence of the field-effect mobility on the dielectric surface hydrophobicity is not due to the orientation of the PTVTF chains. Finally, we determined the temperature dependence of the mobility in order to calculate the activation energy, which is directly related to the surface trap distribution.[35] Figure 8 shows the mobility vs temperature relationships for the various surface-treated layers as Arrhenius plots, and the activation energies were calculated with the Arrhenius equation, $\mu = \mu_0 \exp(-E_A/kT)$. In general, an increase in the thermal activation energy is known to be related to increased widths of the localized trap states in the band gap.[31] However, in the case of an

(31) Shaw, J. M.; Seidler, P. F. *IBM J. Res. Dev.* **2001**, *45*, 3.
(32) Jung, Y.; Cho, T.-Y.; Yoon, D. Y.; Frank, C. W.; Luning, J. *Macromolecules* **2005**, *38*, 867.
(33) Kim, D. H.; Jang, Y.; Park, Y. D.; Cho, K. *Langmuir* **2005**, *21*, 3203.

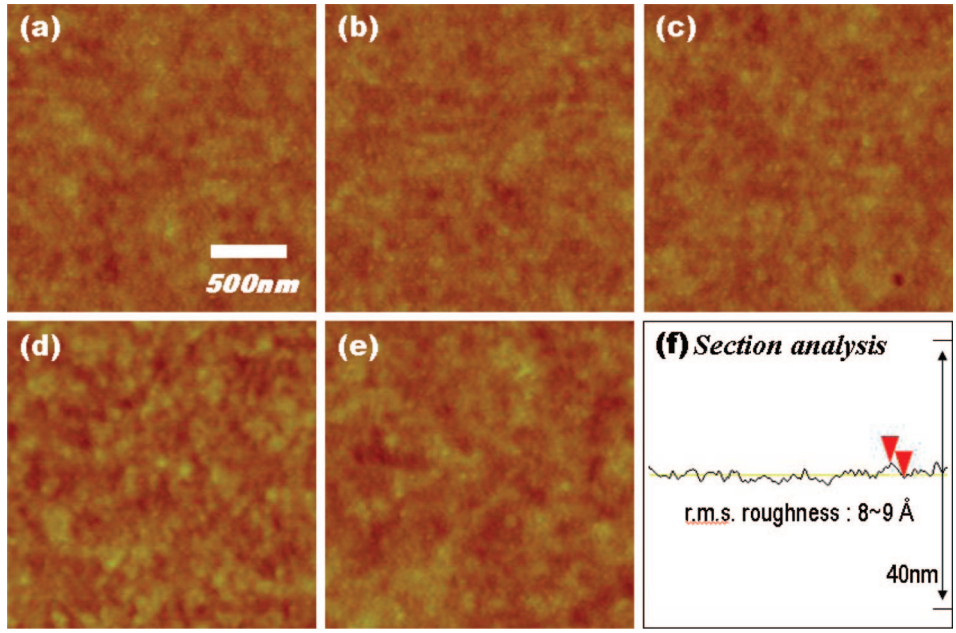

Figure 4. Atomic force microscopy height images for PFTVT films spin-coated onto (a) bare SiO_2, (b) HMDS-treated SiO_2, (c) OTS-treated SiO_2, (d) ODTS-treated SiO_2, (e) PDMS-treated SiO_2. The illustration in f shows a section analysis of the ODTS-treated SiO_2 and confirms its smooth surface morphology.

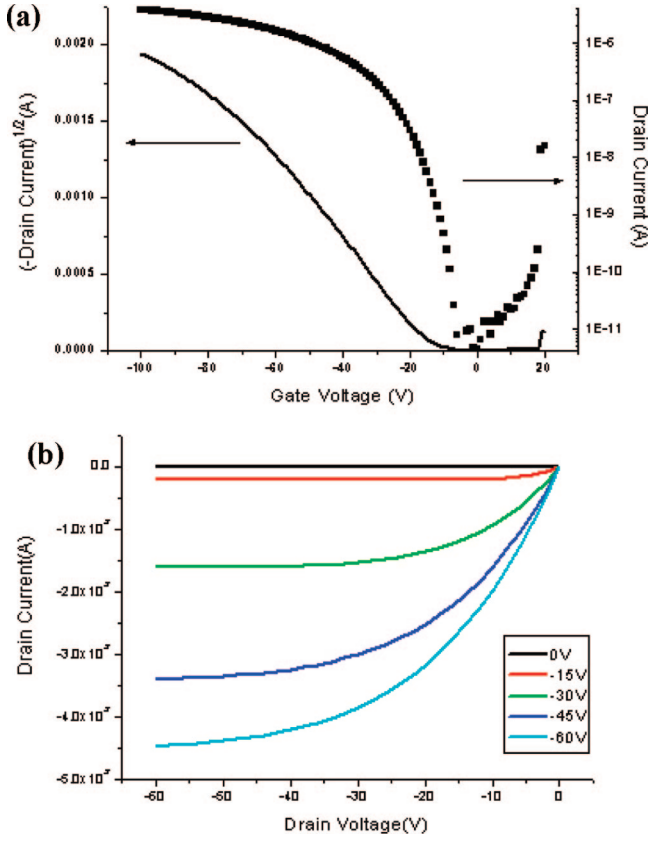

Figure 5. (a) Transfer characteristics of an OTFT with PFTVT coated onto a PDMS-treated SiO_2 dielectric ($L = 75$ μm, $W = 2000$ μm) measured under ambient air. (b) The output characteristics for various gate voltages. Transfer characteristics for the case of other surface treatments used are included in Supporting Information.

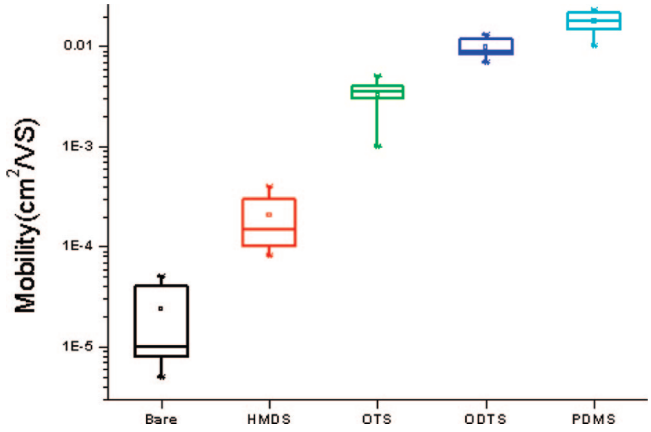

Figure 6. The correlation between the surface treatment of the SiO_2 dielectric layer and the field-effect mobility. Bare SiO_2 has the most hydrophilic surface and the hydrophobicity of the surfaces increases from left to right.

amorphous material, an increase in the activation energy is due to a broadening of the density of states (DOS) due to increased energetic disorder.[36] The activation energy was found to be lowest in the case of the hydrophobic PDMS-treated dielectric (0.055 eV) and to increase as the dielectric surface becomes increasingly hydrophilic. The dipoles of the polar functional groups possibly broaden the DOS around the HOMO level edge of the amorphous semiconductor layer and thus reduce the field-effect mobility. This result is consistent with that for semiconductors on low-k dielectric surfaces, which have lower activation energies than on high-k dielectric surfaces.[18] In addition, the low activation energy (0.07 eV) obtained from the time-of-flight measurements is similar to those of OTFT devices with hydrophobic dielectrics. Since the time-of-flight measurements relate to bulk

(34) Pattison, L. R.; Hexemer, A.; Kramer, E. J.; Krishnan, S.; Petroff, P. M.; Fischer, D. A. *Macromolecules* **2006**, *39*, 2225.
(35) Knipp, D.; Street, R. A.; Volkel, A. R. *Appl. Phys. Lett.* **2004**, *82*, 3907.
(36) Bassler, H. *Phys. Status Solidi B:* **1993**, *175*, 15.
(37) Tanase, C.; Blom, P. W. M.; de Leeuw, D. M.; Meijer, E. J. *Phys. Status Solidi A:* **2004**, *201*, 1236.

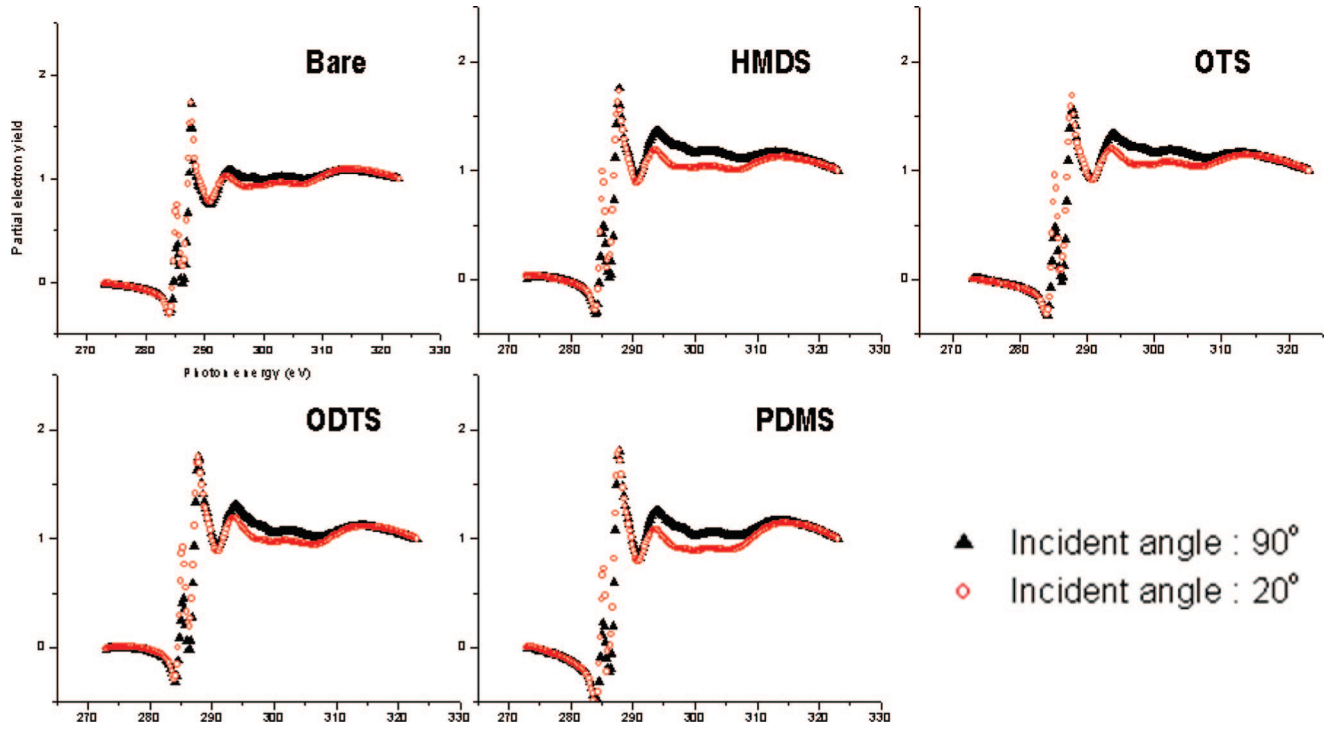

Figure 7. Near edge X-ray absorption fine structure spectra of the C 1s edge of PFTVT films deposited on various surface-treated SiO_2 dielectrics for two different angles of incidence, 90° and 20°.

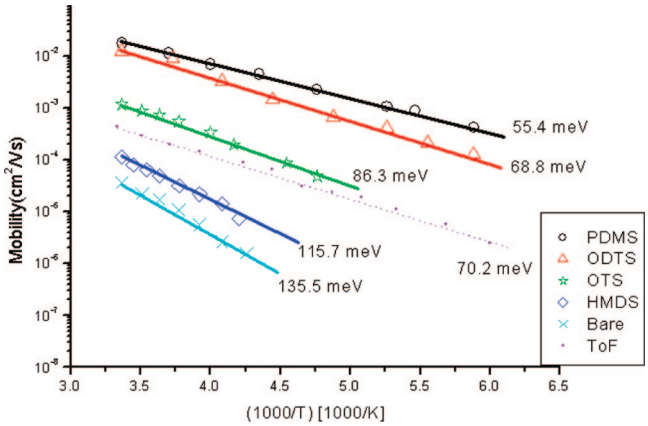

Figure 8. Temperature dependence of the field-effect mobility and the time-of-flight mobility for the various surface-treated dielectrics.

mobility and are not affected by the surface polarity of the dielectric layer, this result also supports our conclusion.

Conclusion

A novel copolymer, poly[(1,2-bis-(2′-thienyl)vinyl-5′,5″-diyl)-*alt*-(9,9-dioctylfluorene-2,7-diyl] (PTVTF), has been synthesized. PTVTF is not susceptible to oxidative doping due to its high ionization energy and is soluble in chloroform and toluene. The amorphous nature of PTVTF thin films was confirmed by the absence of Bragg peaks in the GIXD results, the smooth and amorphous morphology found with AFM, and the absence of any shift in the UV–vis absorption spectrum after annealing. Despite its amorphous nature, a PTVTF thin film transistor was found to have a high mobility of 0.02 cm^2/Vs and a subthreshold slope of 1.7 V $decade^{-1}$. This mobility is an order of magnitude higher than previously reported for amorphous polymeric semiconductors. The reason for this high mobility is not yet clear. We conclude that PTVTF is a promising candidate for low cost, large-area electronics that need good reproducibility of device performance and moderate field-effect mobility. We also found that the mobility of this amorphous polymer improves with increases in the hydrophobicity of the dielectric surface.

Acknowledgment. This work was supported by a grant (F0004020-2006-22) from the Information Display R&D Center, one of the 21st Century Frontier R&D Programs funded by the Ministry of Commerce, Industry and Energy of the Korean Government.

Supporting Information Available: All the FET data for the different surface treatments used; all the difference NEXAFS spectra (90° − 20°). This material is available free of charge via the Internet at http://pubs.acs.org.

CM800447K